PEOPLE'S DEMOCRATIC REPUBLIC OF ALGERIA
MINISTRY OF HIGHER EDUCATION AND SCIENTIFIC RESEARCH
University Amar Telidji- Laghouat

Faculty of Technology

Department of Electrical Engineering

Domain: Sciences and Technology

Field: Electrical Engineering

Option: Electrical Power Systems

MASTER'S DISSERTATION

Presented by: YAGOUBI Abdallah

Theme

Optimal Operation of Distribution Networks Integrating Green Hydrogen Systems for Techno-Economic and Environmental Benefits

Publicly defended before a committee:

Full name	Title	Role
Saliha CHETTIH	Prof.	President
Youcef OUBBATI	M.C.A	Examiner
Salem ARIF	Prof.	Supervisor
Ahmed Tidjani HACHEMI	Dr.	Co-Supervisor

Academic Year 2024-2025

الملخص

يركز هذا العمل على التشغيل الأمثل لشبكة توزيع كهربائية مدمجة بألواح شمسية، توربينات رياح، ونظام تخزين للهيدروجين الأخضر. تم صياغة مسألة تحسين متعددة الأهداف بهدف تقليل خسائر الطاقة، انحراف الجهد، تكلفة التشغيل، والانبعاثات الملوثة. تم استخدام خوارزمية صقور هاريس لتحديد المواقع والأحجام المثلى لمصادر الطاقة. تم اعتماد شبكة اختبار المكونة من 33 عقدة لتقييم المنهجية المقترحة عبر ثلاث سيناريوهات. أظهرت النتائج أن دمج الطاقات المتجددة مع نظام الهيدروجين الأخضر يُحسِّن من أداء الشبكة واستدامتها. كما أثبتت خوارزمية صقور هاري فعاليتها في حل هذا النوع من المسائل.

الكلمات المفتاحية

الهيدروجين الأخضر، الطاقة الشمسية، طاقة الرياح، شبكة التوزيع، خوارزمية صقور هاريس

Abstract

This work focuses on the optimal operation of a distribution network integrating photovoltaic panels, wind turbines, and green hydrogen storage systems. A multi objective optimization problem is formulated to minimize power losses, voltage deviation, operational costs, and emissions. The Harris Hawks Optimization (HHO) algorithm is applied to determine the optimal placement and sizing of energy components. The IEEE 33 bus test system is used to validate the proposed approach through three scenarios. Results show that the integration of renewable and hydrogen-based sources improves network performance and sustainability. The HHO algorithm proves effective in solving the optimization problem efficiently.

Index terms

Green Hydrogen, Photovoltaic, Wind, Distribution Network, Harris Hawks Optimization

Résumé

Ce travail porte sur le fonctionnement optimale d'un réseau de distribution intégrant des panneaux photovoltaïques, des éoliennes et un système de stockage à hydrogène vert. Un problème d'optimisation multi-objectif est formulé afin de minimiser les pertes de puissance, la déviation de tension, le coût d'exploitation et les émissions polluantes. L'algorithme d'optimisation des faucons de Harris (HHO) est utilisé pour déterminer l'emplacement et le dimensionnement optimaux des sources d'énergie. Le réseau test IEEE à 33 nœuds est utilisé pour valider la méthode à travers trois scénarios. Les résultats montrent que l'intégration des énergies renouvelables et de l'hydrogène vert améliore les performances et la durabilité du réseau. L'algorithme HHO s'avère efficace pour résoudre ce type de problème.

Mots clés

Hydrogène Vert, Photovoltaïque, Éolien, Réseau de Distribution, Optimisation de Harris Hawks

Acknowledgements

First and foremost, I would like to thank **God Almighty** for granting me the strength, patience, and determination to complete this work.

I express my deepest gratitude to my parents for their unconditional love, unwavering support, and constant encouragement, which have enabled me to persevere through challenges. I sincerely hope that this work reflects their trust and dedication.

I would also like to extend my heartfelt thanks to my supervisor, **Professor Salem Arif,** for his valuable guidance, availability, and insightful advice throughout this project.

My sincere appreciation goes as well to my co-supervisor, **Dr. Ahmed Tidjani Hachemi,** for his support, constructive feedback, and encouragement, which have greatly contributed to the successful completion of this work.

I would also like to thank the members of the examination committee, **Professor Saliha Chettih** and Associate **Professor Youcef Oubbati**, for their time and valuable insights during the defense of this dissertation.

I am also grateful to all the professors at the university for the quality of their teaching, their commitment, and the invaluable knowledge they have shared with me over the course of my academic journey.

A special thank you to my family for their comforting presence and emotional support, which have been truly invaluable.

Finally, I would like to thank my friends, who have supported me with kindness since the very beginning of my time at the university. I am grateful to everyone who has helped me, directly or indirectly, throughout this meaningful experience.

Dedication

To my dearest parents, your unconditional love, endless sacrifices, and unwavering faith in me have been the pillars of my strength. I owe you everything, and I hope this achievement makes you proud.

To my beloved family, thank you for your constant encouragement, patience, and emotional support. You have always been my source of inspiration and resilience.

To my beloved brother Sidali, your support, advice, and constant belief in me have meant the world. Thank you for always being there through the highs and lows. This success is also yours.

To my respected supervisor, Pr. Arif Salem, I extend my heartfelt thanks for your patience, wise guidance, and continuous support throughout this journey. Your mentorship has had a lasting impact on my academic and personal growth.

To my esteemed co-supervisor, Dr. Hachemi Ahmed Tidjani, I am deeply grateful for your insightful advice, valuable time, and encouragement, which played a crucial role in shaping this research.

To my dear friends and colleagues, thank you for your companionship, motivation, and the moments of joy and strength we shared along the way.

This work is a reflection of the support, care, and wisdom I received from all of you.

Contents

Abbreviations and Symbols List

Abbreviations list:

BFS	: Backward/Forward Sweep
RES	: Renewable Energy Sources
PV	: Photovoltaic
WT	: Wind Turbine
GHS	: Green Hydrogen System
FC	: Fuel Cell
HHO	: Harris Hawks Optimization
IEEE	: Institute of Electrical and Engineers
DG	: Distributed Generation
BIBC	: Bus Injection to Branch Current matrix

Symbols list:

A_{PV}	: Total area used by the PV array
T_c	: Cell temperature in degrees Celsius
T_a	: Ambient temperature in degrees Celsius
P_{EL}	: Power absorbed by the electrolyzer
η_E	: Efficiency of the electrolyzer
HHV_{H_2}	: Higher Heating Value of Hydrogen
η_{FC}	: Efficiency of the Fuel Cell
$TRPL$	: Total Real Power Losses
C	: Total Operation Cost
TE	: Total Emissions
TVD	: Total Voltage Deviation
R_i	: Resistance of branch i
P_{Grid}	: Power from the grid
ε_{Loss}	: Cost per kilowatt-hour of power losses
C_{PV}^{inst}	: Installation costs associated with the PV system
$O\&M$	: Operation and Maintenance
$C_{PV}^{O\&M}$	: Ongoing operations and maintenance costs of the PV system
$\mu_{PV}^{O\&M}$	: Cost per kilowatt-hour for operations and maintenance
P_{Ele} , P_{FC}	: Power of the electrolyzer and fuel cell

S_{HT}	: Storage of hydrogen tank
$P_{Loss,i}$, $Q_{Loss,i}$	: Active and reactive power losses
$P_{Load,i}$, $Q_{Load,i}$	: Reactive and active power required by load
Q_S, P_S	: System reactive and active power supply
P_{PV}	: Photovoltaic Power
P_{WT}	: Wind turbine Power
P_{Ele}	: Electrolyzer Power
P_{FC}	: Fuel Cell Power

List of Figures

List of Tables

General Introduction

The global energy system is undergoing major changes to become more sustainable. This shift is driven by the urgent need to combat climate change, enhance energy security, and meet the growing demand for electricity. Electrical distribution networks (EDNs), which connect centralized power plants to end users, play a key role in this transition. However, traditional EDNs face several challenges, including voltage instability, high energy losses, and difficulties integrating renewable energy sources (RES) such as solar and wind, which are inherently intermittent.

Moreover, the growing use of distributed energy resources (DERs), energy storage systems, and decarbonization targets requires advanced tools for system analysis and optimization to ensure reliable, cost-effective, and environmentally friendly operation.

This work focuses on the optimal operation of a distribution network that incorporates renewable energy sources and a green hydrogen storage system. A comprehensive multi-objective optimization problem is formulated to minimize power losses, voltage deviations, operational costs, and pollutant emissions.

The IEEE 33-bus test system is used as a case study, and the Harris Hawks Optimization (HHO) algorithm is employed to determine the best locations, sizes, and operating strategies for the integrated energy components.

This research bridges theoretical rigor with practical application, using MATLAB simulations and metaheuristic optimization techniques to enhance the design and operation of future-proof EDNs. It addresses limitations in traditional power flow methods for radial networks and demonstrates the synergy between RES and hydrogen storage. This work contributes to the global effort to develop resilient, low-carbon energy systems.

This master's thesis addresses these challenges through a comprehensive study structured into three interconnected chapters:

Chapter I establishes the fundamentals of EDNs, highlighting their structural differences from transmission systems and introducing key concepts such as power flow analysis, branch and load modeling, and the integration of RES and storage technologies.

Chapter II develops a detailed mathematical framework for modeling photovoltaic (PV) systems, wind turbines (WTs), and green hydrogen storage (GHS) components. It formulates a multi-objective optimization problem to minimize real power losses, operational costs, voltage deviations, and emissions, using the Harris Hawks Optimization (HHO) algorithm.

Chapter III validates the proposed models and optimization approach using the IEEE 33-bus test system under three operational scenarios, demonstrating the techno-economic and environmental benefits of integrating RES and GHS.

Chapter I
Advanced Analysis of Electrical Distribution Networks with Renewable Sources and Storage

1.1 Introduction

The electrical distribution network plays a critical role as the final link between centralized generation and end users. It ensures that power generated from diverse sources including conventional and renewable systems is delivered reliably and efficiently to residential, commercial, and industrial consumers. As energy systems evolve toward more decentralized and sustainable models, the distribution network has become increasingly important in integrating technologies such as solar panels, wind turbines, and green hydrogen systems. Its operation and planning are key to ensuring voltage stability, minimizing losses, and supporting the integration of distributed energy resources.

In this context, power flow analysis becomes a fundamental and indispensable tool for assessing the steady-state behavior of electrical systems. It enables the determination of key performance indicators such as bus voltages (magnitudes and angles), real and reactive power flows, and line losses. Load flow studies are essential for the continuous evaluation of existing power networks and for effective planning of future expansions to meet increasing demand.

These studies are also critical for equipment selection and system design, including switchgear, transformer, and cable sizing. Furthermore, they help ensure proper voltage profiles under various operating conditions, ranging from heavily loaded to lightly loaded scenarios. Load flow analysis also supports decisions related to the optimal placement and sizing of distributed generation (DG) and capacitor banks for power factor correction. Importantly, load flow results often serve as the foundation for further system studies and simulations.

Over recent decades, several efficient and widely used power flow methods have been developed for transmission systems, such as:

- Gauss-Seidel method with admittance matrix (YGS)
- Gauss-Seidel method with impedance matrix (ZGS)
- Newton Raphson (NR) method
- Decoupled Newton Raphson (DNR)
- Fast Decoupled Newton Raphson (FDNR)

However, the analysis of distribution systems poses unique challenges. While transmission networks are typically meshed with a high X/R ratio, distribution networks are usually radial in structure and characterized by a high R/X ratio. These differences render

conventional power flow methods less effective or non-convergent when applied to distribution systems. For this reason, it is essential to understand the specific nature and components of distribution networks before performing power flow analysis within them.

1.2 Fundamentals of Distribution Networks

The distribution system is the final link between power generation and end-users. It connects the transmission network to consumers through substations and feeders, ensuring the delivery of electricity at medium or low voltage levels. Unlike transmission systems, which are typically meshed and optimized for bulk energy transfer, distribution networks generally follow a radial structure and are designed for shorter distances and lower power capacities. Due to these characteristics, they are more affected by voltage drops and power losses, especially under variable load conditions. Understanding the specific structure and operation of distribution systems is essential before addressing their development and optimization.

1.3 Modeling of Network Branches and Loads

1.3.1 Branch Modeling

The radial distribution network consists of a set of branches. Each branch is modeled as a series combination of resistance and pure inductance. The impedance of any branch i in the network, as shown in Figure 1.1, is expressed as follows:

$$Z_i = R_i + jX_i \tag{1.1}$$

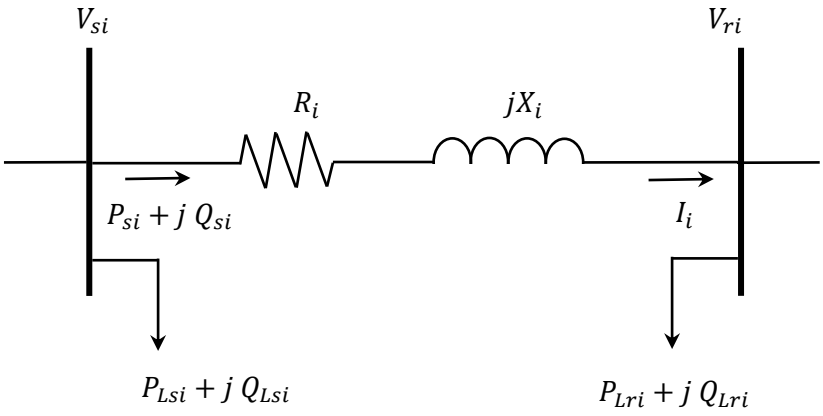

Figure 1.1: Representation of two nodes in the radial EDN.

1.3.2 Load Modeling

Load is the most uncertain parameter in the distribution electrical network; it is constantly variable. Over a year, the load can vary significantly from season to season, day to day, and hour to hour. It is the most sensitive parameter that can influence the solution to the EDN planning problem. Most researchers in the literature assume a constant load model in their EDN planning studies. Decisions and results based on this assumption are not technically feasible for real distribution systems where the load is not constant. In this study, to achieve an effective analysis, two types of loads will be considered:

1.3.2.1 Periodic Constant Load Model

This load model is characterized by relatively constant electrical energy consumption during certain time intervals, with a variation that depends very little on weather conditions. The energy demand is fairly stable from day to day and season to season. Consumption levels typically change 1–3 times daily. Large consumers and many industrial customers exhibit this load model. Mathematically, the active and reactive powers during each level of demand α are calculated respectively by equations (1.2) and (I.3):

$$P_{L\alpha} = P_{L0} \times D_{\alpha} \tag{1.2}$$

$$Q_{L\alpha} = Q_{L0} \times D_{\alpha} \tag{1.3}$$

Where, P_{L0} and Q_{L0} are the nominal active and reactive powers, D_{α} is the load level factor.

1.3.2.2 Static Load Model

The static model represents the characteristics of loads in steady-state conditions. It generally describes the relationship between active and reactive power with the voltage level over a specified period of time. In this load model, active and reactive powers are represented in exponential form. This model is also used to approximate the dynamic characteristics of loads. The load model is expressed by the following equations [1]:

$$P_{Li} = P_{L0}\left(\frac{V_i}{V_0}\right)^{\alpha} \quad (1.4)$$

$$Q_{Li} = Q_{L0}\left(\frac{V_i}{V_0}\right)^{\beta} \quad (1.5)$$

Where, V_0 is the nominal voltage,P_{Li} and Q_{Li} are the active and reactive power of the load at node i for a voltage equal to V_i.The coefficients α and β determine the nature of the load.

The values of the coefficients α and β depend on the aggregated characteristics of the load components. When both coefficients α and β are equal to 0, the load behaves like a constant power load, which means the power does not vary when the voltage changes. On the other hand, if the coefficients are equal to 1, the load behaves like a constant current load, where the power varies proportionally with the voltage. If the coefficients are equal to 2, the load behaves like a constant impedance load, where the power varies proportionally with the square of the voltage.

1.4 Power Flow Calculation in Distribution Network

Power flow calculations, or load distribution calculations, in an electric network planning problem, are crucial for determining energy losses for any network states that may arise and ensuring that these states satisfy the network's operational constraints.

In the context of electric network planning, power flow calculations are a repetitive and essential task, especially when using optimization methods, as will be employed later in this work. The use of a fast and accurate power flow calculation method is vital to accomplish this task.

However, electric distribution networks have certain typical characteristics that differ from transmission networks. They are characterized by [2]:

- Generally radial or weakly meshed structure,
- High resistance-to-reactance ratio ,
- Large number of branches and nodes,
- Unbalanced loads.

Various algorithms have been developed in the literature [3, 4], specifically designed to solve the power flow problem in electric distribution networks. The most common algorithm is the Backward/Forward Sweep Algorithm [5], which will be explained in the following section.

1.4.1 Backward/Forward Sweep Algorithm

Over the past decades, various methods based on the Backward/Forward Sweep (BFS) Algorithm have been developed in several studies reported in the literature [6-8]. This was done to accelerate the power flow calculation in EDNs and achieve good convergence by avoiding the simultaneous solution of systems of equations and the use of large matrices. Unlike common methods such as Gauss-Seidel and Newton-Raphson, the sweep algorithm has the advantage of requiring less computational effort and time.

In this subsection, we will explain the iterative algorithm principle of the Backward/Forward Sweep method. This algorithm calculates the current on each branch and the voltage for each node. At each iteration, two sweeps are executed:

- Backward Sweep: Determines the currents in the branches of the network using the first Kirchhoff's law.
- Forward Sweep: Calculates the node voltages by computing voltage drops along the branches.

The BFS algorithm is characterized by its simplicity, speed, and accuracy. It operates in three steps.

Step 1: Calculation of Injection Currents

After reading the data from the EDN and initializing all node voltages, the injected current at each node is calculated based on the power absorbed by the connected load and the voltage at that node. For a node i, the injected current can be expressed as follows:

$$I_{Li} = \frac{S_{Li}^*}{V_i^*} \tag{1.6}$$

Where, S_{Li}^{*} is the complex power absorbed by the load at node i.V_i^{*} is the complex voltage at node i.

Step 2: Backward Sweep

During the second step, a backward sweep is performed in a descending manner from the terminal nodes of the network towards the source node (source substation) to calculate the branch currents by summing the currents at different nodes of the network. The branch currents are calculated using the formula (1.7):

$$[I] = [BIBC][I_L] \tag{1.7}$$

Where, I represents the vector of branch currents. $BIBC$ is the matrix of injected currents at nodes (Bus Injection Branch Current), which is an upper triangular matrix containing only 0 and 1 values. I_L denotes the vector of injected currents at the terminal nodes of the network.

Construction of the BIBC Matrix [9, 10]:

1. Identification of Nodes and Branches: Begin by identifying all nodes and branches within the electrical network. Nodes represent points of connection, while branches denote conductive elements such as transmission lines and transformers.
2. Assignment of Node Indices: Assign unique indices to each node within the network. These indices will serve to identify the rows and columns of the BIBC matrix.
3. Formulation of Kirchhoff's Current Law (KCL) Equations: Write KCL equations for each node in the network, expressing the sum of currents entering and leaving the node as zero for a stable system.
4. Matrix Representation of KCL Equations: Represent the KCL equations in matrix form to create the BIBC matrix. This matrix is square with dimensions corresponding to the number of nodes in the network.
5. Determination of Matrix Elements: Populate the elements of the BIBC matrix based on the network's connectivity.
    - If there exists a direct path or connection from node i to node j, assign a value of 1 to the corresponding element in the BIBC matrix.
    - If no direct connection exists between nodes i and j, assign a value of 0.

6. Structuring the BIBC Matrix: The BIBC matrix typically exhibits an upper triangular structure due to the directional flow of currents in the network.

Step 3: Forward Sweep

During the third step, a forward sweep is performed in an ascending manner from the source node towards the terminal nodes of the network to calculate the voltage for each node by computing the voltage drop on each branch.

$$V_{ri} = V_{si} - Z_i \cdot I_i, \qquad i = 1, 2, \dots, NT \tag{1.8}$$

Where, si and ri are the start and end of branch i, Z_i is the series impedance of branch i, NT is the number of branches in the EDN.

1.5 Renewable Energy Sources and Storage Technologies

The transition toward sustainable power systems relies heavily on the integration of renewable energy sources and efficient storage technologies. These components play a vital role in reducing greenhouse gas emissions, enhancing energy security, and supporting the optimal operation of distribution networks.

1.5.1 Types of Renewable Energy Sources

Several renewable energy sources can be integrated into modern distribution systems, including:

1.5.1.1 Solar Energy

Converts sunlight directly into electricity using solar panels. It is widely used due to its scalability and decreasing cost. The advantages and disadvantages associated with solar photovoltaic systems can be summarized in Table 1.1.

Table 1.1 Advantages and disadvantages of photovoltaic

Advantages	Disadvantages
No emissions	Non-firm power generation
No fuel cost	Significant capital investment required
No noise impact	Low efficiency
Scalable capacity expansion	Possible requiring large areas
Capable of exporting reactive power	Limited to sun-rich regions

1.5.1.2 Wind Energy

Uses wind turbines to convert wind kinetic energy into electrical energy. Wind power is often used in areas with strong and consistent wind patterns. The advantages and disadvantages associated with wind turbine units are summarized in Table 1.2 [11].

Table 1.2 Advantages and disadvantages of wind turbine

Advantages	Disadvantages
No emissions	Intermittent power generation
Low operation and maintenance cost	Low capacity factor
No fuel cost	Possible high noise level
Capable of exporting reactive power	Difficult to predict power generation

1.5.1.3 Hydropower

Generates electricity by harnessing the energy of flowing or falling water. Although more common in large-scale systems, small hydro plants can be integrated into local networks.

1.5.1.4 Biomass Energy

Produced from organic materials such as agricultural waste or forestry residues. Biomass can be used for electricity generation or heating.

1.5.2 Energy Storage Technologies

Storage systems are essential for balancing supply and demand, enhancing grid stability, and enabling the use of intermittent renewable sources. The main storage technologies include:

1.5.2.1 Battery Energy Storage Systems

Lithium-ion batteries are the most common. They provide fast response and high efficiency for short- to medium-term storage.

1.5.2.2 Green Hydrogen Systems

Excess electricity from renewable sources is used to produce hydrogen through electrolysis. The hydrogen is stored and later converted back into electricity using fuel cells, offering long-term, clean energy storage. The advantages and disadvantages associated with GHS units are summarized in Table 1.3.

Table 1.3 Advantages and disadvantages of GHS

Advantages	Disadvantages
No emissions	Costly production
Long-term energy storage capability	High infrastructure investment
Sector coupling capability	Low efficiency
Versatile energy applications	Complex and risky hydrogen handling

1.5.2.3 Pumped Hydro Storage

Excess electricity is used to pump water to a higher elevation. When electricity is needed, the water is released to generate power through turbines.

1.5.2.4 Thermal Energy Storage

Stores energy in the form of heat, typically using molten salts or water, and is mainly used in conjunction with concentrated solar power (CSP) systems.

1.5.2.5 Flywheels and Supercapacitors

Used for short-duration, high-power applications to stabilize voltage and frequency in the grid.

1.6 Conclusion

In this chapter, we explored the fundamentals of electrical distribution networks, highlighting their structural differences from transmission systems and their critical role in modern power systems. We discussed load and branch modeling, introduced different load types, and emphasized the importance of accurate power flow analysis. The Backward/Forward Sweep algorithm was presented as an effective method for solving power flow in radial systems.

Finally, we examined the main types of renewable energy sources and energy storage technologies, underlining their importance in improving the efficiency, reliability, and sustainability of distribution networks.

Chapter II

System Component Modeling and Optimization

2.1 Introduction

In the pursuit of sustainable and efficient energy systems, the integration of renewable energy sources and advanced storage technologies has become increasingly vital. To address this, Chapter II presents a detailed modeling framework for the primary components of a hybrid power distribution system, including photovoltaic (PV) systems, wind turbines (WT), and hydrogen storage units. These components are mathematically characterized to capture their dynamic performance and interaction with the grid. In addition to system modeling, this chapter formulates a comprehensive multi-objective optimization problem aimed at minimizing real power losses, operation costs, voltage deviations, and pollutant emissions. The chapter concludes by introducing the Harris Hawks Optimization (HHO) algorithm as an effective metaheuristic tool for solving the problem under various operational and regulatory constraints.

2.2 Modeling the Different Systems

2.2.1 PV System

The power output of a PV system can be determined using the following formula:

$$T_c(h) = T_a(h) + \frac{I(h)}{800} \cdot (NOCT - 20) \tag{2.1}$$

$$P_{PV}(h) = A_{PV} \cdot \eta_{PV}(h) \cdot I(h) \tag{2.2}$$

The total area used by the PV array, labeled as A_{PV} in (m^2), is multiplied by the conversion efficiency of the PV panels, η_{PV}, to get the output produced by the PV, expressed as P_{PV} (kW). The cell temperature is expressed in degrees Celsius as T_c. The ambient temperature in degrees Celsius is represented by T_a. I is the solar insolation in (kW/m^2). The instantaneous efficiency of PV panels η_{PV} is obtained using the following equation [12]:

$$\eta_{PV}(h) = \eta_r \cdot \eta_t \times \left[1 - \gamma \cdot (T_a(h) - T_r) - \gamma \cdot I(h) \cdot \left(\frac{NOCT - 20}{800}\right) \cdot (1 - \eta_r \cdot \eta_t)\right] \tag{2.3}$$

where η_t is the effectiveness of the maximum power point tracking device, and η_r is the PV panels' reference efficiency. It also takes into account the temperature coefficient of efficiency γ, which for silicon cells, normally ranges from 0.004 to 0.006 per (℃$^{-1}$). Nominal operating cell temperature $NOCT$ in (℃), reference temperature T_r in (℃) for PV cells, and ambient temperature T_a in (℃) are also considered.

2.2.2 WT System

The WT energy output (P_{WT}) can be determined using the following formula:

$$P_{WT}(V) = \begin{cases} 0 & for \quad V < V_i \; and \; V > V_o \\ P_{rated\_WT}\left(\dfrac{V - V_i}{V_r - V_i}\right) & for \quad (V_i \leq V \leq V_r) \\ P_{rated\_WT} & for \quad (V_r < V \leq V_o) \end{cases} \tag{2.4}$$

The used wind turbine has a rated power of 250 kW, a rated velocity V_r of 15 m/s, a cut-out speed V_o of 25 m/s, and a cut-in speed V_i of 2.5 m/s [12].

2.2.3 Hydrogen Storage System

This system comprises three main components: an electrolyzer, a hydrogen tank, and a fuel cell.

The electrolyzer converts surplus electricity or grid-supplied power into hydrogen. It consists of two electrodes (anode and cathode) and an electrolyte, which splits water into hydrogen and oxygen as per the following equation [13]:

$$H_2O + \; Power = H_2 + \frac{1}{2}O_2 \tag{2.5}$$

The mass of hydrogen produced by the electrolyzer is calculated using the formula:

$$M(t) = \frac{P_{EL}(t) \times \eta_E}{HHV_{H_2}} \tag{2.6}$$

where $P_{EL}(t)$ represents the power absorbed by the electrolyzer, η_E is the efficiency of the electrolyzer, and HHV_{H_2} refers to the higher heating value of hydrogen, which is 39.4 kWh/kg [14].

The fuel cell (FC) converts stored hydrogen into electricity to address energy deficits. The reaction within the FC is represented as follows [15] :

$$2H_2 + O_2 = 2H_2O + Power \tag{2.7}$$

The power generated by the FC is given by:

$$P_{FC}(t) = P_{FC-H}(t) \times \eta_{FC} \tag{2.8}$$

where η_{FC} represents the efficiency of the FC, and $P_{FC-H}(t)$ is the power derived from hydrogen supplied to the FC.

The hydrogen delivered by the electrolyzer is stored in a tank designed to hold a specific amount of hydrogen. This tank supplies hydrogen to the fuel cell for electricity production. The hydrogen state in the tank is calculated as follows:

$$E_T(t) = E_T(t-1) + P_{EL}(t) \times \eta_{\mathrm{E}} - P_{FC}(t)/\eta_{FC} \tag{2.9}$$

This system links power generation to end-users via substations and feeders, delivering electricity at medium/low voltage levels. Unlike transmission systems, which are typically meshed and optimized for bulk energy transfer, distribution networks are typically radial, designed for shorter distances and lower power capacities. Due to these characteristics, they are more susceptible to voltage drops and power losses under variable loads. Understanding their specific structure and operation is essential before addressing their development and optimization.

2.3 Problem Formulation

This section explores the formulation of key performance indicators for optimizing a power distribution system. The focus includes Total Real Power Losses (*TRPL*), which asses system efficiency, Total Operation Cost (C), which calculates the comprehensive costs of running the network, Total Voltage Deviation (*TVD*) for network stability, and Total Emission (*TE*) reflecting the environmental impact. Each parameter is calculated using specific formulas to guide strategies for reducing costs, emissions, and improving system reliability and efficiency.

2.3.1 Objective Function

2.3.1.1 Total Real Power Losses

Reducing Total Real Power Losses (TRPL) is important as it directly impacts the efficiency and economic operation of the power distribution system, aligning with our goal to enhance network performance and reduce operational costs. TRPL can be represented using the following equation [16, 17]:

$$TRPL = \sum_{t=1}^{24} \sum_{i=1}^{NT} P_{Loss(i,t)} \tag{2.10}$$

$$P_{Loss(i,t)} = \left|I_{(i,t)}\right|^2 R_i = \left(\frac{P_{(i,t)}^2 + Q_{(i,t)}^2}{\left|V_{s(i,t)}\right|^2}\right) R_i \tag{2.11}$$

where $I_{(i,t)}$ is the current on the branch i, R_i is the resistance of branch i, $P_{(i,t)}$ and $Q_{(i,t)}$ are the real and reactive power flows on the branch i, respectively, and $V_{s(i,t)}$ is the voltage at the sending node of the branch i, $NT$is the number of branches.

2.3.1.2 Total Operation Cost

The total operation cost for a distribution network is determined by Equation (2.12), which summarizes the key components of operational expenses. These include the cost of the DN C_{tot}, which involves the WT system cost C_{Wind}, photovoltaic system cost C_{PV}, cost of energy procurement C_{Grid}, cost of energy losses C_{Loss}, and cost of hydrogen storage C_H. The total cost is formulated as follows:

$$C_{tot} = min(C_{Wind} + C_{PV} + C_{Grid} + C_{Loss} + C_H) \tag{2.12}$$

In which,

$$C_{Grid} = \sum_{t=1}^{24} P_{Grid(t)} \times \vartheta_{Grid(t)} \tag{2.13}$$

$P_{Grid(t)}$ represents the power from the grid at each hour t, and $\vartheta_{Grid(t)}$ denotes the price of grid electricity at that hour. These factors are used to calculate the hourly cost of grid electricity, which is then summed up for all 24 hours of the day to represent the day cost of electricity drawn from the grid.

$$C_{Loss} = \varepsilon_{Loss} \times \sum_{t=1}^{24} P_{T\_Loss(t)} \tag{2.14}$$

Where ε_{Loss} is the cost per kilowatt-hour of power losses, set at 0.06 USD/kWh [18]. $P_{T\_Loss(t)}$ represents the power losses at each hour t over a 24-hour period.

$$C_{PV} = C_{PV}^{inst} + C_{PV}^{O\&M} \tag{2.15}$$

Where C_{PV}^{inst} represents the installation costs associated with the PV system, and $C_{PV}^{O\&M}$ refers to the ongoing operations and maintenance costs of the PV system.

$$C_{PV}^{O\&M} = \mu_{PV}^{O\&M} \times \sum_{t=1}^{24} \sum_{i=1}^{N_{PV}} P_{PV(i,t)} \tag{2.16}$$

$$C_{PV}^{inst.} = CF \times U_{PV} \times \sum_{i=1}^{N_{PV}} P_{rated\_PV(i)} \tag{2.17}$$

Where $\mu_{PV}^{O\&M}$ is the cost per kilowatt-hour for operations and maintenance, valued at 0.01 USD/kWh [19] and $P_{PV(i,t)}$ represents the power output from the i^{th} photovoltaic unit at time t. N_{PV} represents the number of photovoltaic units. For the installation costs, CF denotes the capital recovery factor, U_{PV} is the unit cost per rated power, set at 770 USD/kW, and $P_{rated\_PV(i)}$ is the rated power of the i^{th} PV system [20].

$$C_{WT} = C_{WT}^{inst.} + C_{WT}^{O\&M} \tag{2.18}$$

Where $C_{WT}^{O\&M}$ is the wind's maintenance and operating costs and $C_{WT}^{inst.}$ is the cost of installing the WT.

$$C_{WT}^{O\&M} = U_{WT}^{O\&M} \times \sum_{i=1}^{N_{WT}} \sum_{t=1}^{24} P_{WT(i,t)} \tag{2.19}$$

where the maintenance and operating expenses for WTs are represented by $U_{WT}^{O\&M}$ valued at 0.01 USD/kWh. N_{WT} is the number of WTs.

$$C_{WT}^{inst.} = CF \times U_{WT} \times \sum_{i=1}^{N_{WT}} P_{rated\_WT(i)} \tag{2.20}$$

where U_{WT} stand for the corresponding purchasing costs of WTs set at 1400 USD/kW. The rated generated power of the i^{th} WT system is denoted by $P_{rated\_WT(i)}$. $P_{WT(i,t)}$ denote the hourly produced power of the i^{th} WT system.

The capital recovery factor is represented by the following equation:

$$CF = \frac{ir \times (1+ir)^N}{(1+ir)^N - 1} \tag{2.21}$$

where ir represents the interest rate, and N denotes the number of periods over which the investment is amortized.

The Hydrogen storage cost including its installation as well as operation and maintenance costs is represented by:

$$C_H = C_H^{inst.} + C_H^{O\&M} \tag{2.22}$$

The operation and maintenance cost of this storage is expressed as [21]:

$$C_H^{O\&M} = \sum_{t=1}^{24} \sum_{i=1}^{Nsys} \left[P_{Ele(i,t)} \times \mu_{Ele}^{O\&M} + S_{HT(i,t)} \times \mu_{HT}^{O\&M} + P_{FC(i,t)} \times \mu_{FC}^{O\&M}\right] \tag{2.23}$$

The installation cost of this storage system is formulated as [21]:

$$C_H^{inst.} = CF \times [P_{Ele} \times U_{Ele} + S_{HT} \times U_{HT} + P_{FC} \times U_{FC}] \tag{2.24}$$

where $P_{\mathrm{Ele}(i,t)}$, $S_{HT(i,t)}$, and $P_{FC(i,t)}$ represent the power and storage contributions at time t for the electrolyzer, hydrogen tank, and fuel cell, respectively, while $\mu_{Ele}^{O\&M}$, $\mu_{HT}^{O\&M}$, and $\mu_{FC}^{O\&M}$

denote their respective operation and maintenance cost coefficients valued at 0.2 USD/kWh. U_{Ele}, U_{HT} *and* U_{FC} *are* the unit costs per rated power for the electrolyzer, hydrogen tank, and fuel cell, respectively, set at 150 USD/kW, 300 USD/kW and 600 USD/kW.

2.3.1.3 Total Voltage Deviation

Reducing voltage deviation is crucial for enhancing the performance of electrical networks, particularly in stabilizing network voltage levels. This is quantified by the Total Voltage Deviation (TVD), which is given by the following equation [22-24]:

$$TVD = \sum_{t=1}^{24} \sum_{i=1}^{NB} \left| \left(V_{(i,t)} - 1 \right) \right| \tag{2.25}$$

where NB represents the total number of buses or nodes in the network, and $V_{(i,t)}$ denotes the Voltage magnitude (per unit) at node i at time t.

2.3.1.4 Total Emission

Reducing Total Emission (TE) is crucial in our study as it directly relates to environmental sustainability and compliance with regulatory standards for air quality. The primary pollutants involved in this calculation are carbon dioxide (CO_2), nitrogen oxides (NO_x), and sulfur dioxide (SO_2), which are critical contributors to atmospheric pollution. These emissions are particularly significant in the context of power generation from grid-supplied electricity. Total Emission is represented by the following equation, with emissions measured in kilograms (kg) [25].

$$TE = \sum_{t=1}^{24} P_{Grid(t)} \times \left(CO_2^{Grid} + NO_x^{Grid} + SO_2^{Grid} \right) \tag{2.26}$$

Where the emissions factors for CO_2 are 921.25 kg/MWh, for NO_x are 2.2952 kg/MWh, and for SO_2 are 3.5834 kg/MWh. $P_{Grid(t)}$ is converted to MW to align with kg/MWh emission factors.

In this study, the weighted penalty summation method was used to solve the multi-objective problem. This method involves combining the individual objective functions into a single aggregated objective function by assigning a weight to each objective, as described below:

$$\min(MOF) = \min(\varepsilon_1 F_1 + \varepsilon_2 F_2 + \varepsilon_3 F_3 + \varepsilon_4 F_4) \tag{2.27}$$

$$F_1 = \frac{TRPL_{after}}{TRPL_{before}} \tag{2.28}$$

$$F_2 = \frac{C_{after}}{C_{before}} \tag{2.29}$$

$$F_3 = \frac{TVD_{after}}{TVD_{before}} \tag{2.30}$$

$$F_4 = \frac{TE_{after}}{TE_{before}} \tag{2.31}$$

Where the terms $before$ and $after$ refer to the values of parameters before and after the implementation of improvements, respectively. Additionally, the weights $\varepsilon_1, \varepsilon_2, \varepsilon_3, \varepsilon_4$ are all set to 0.25, equally distributing the importance across all objective functions F_1, F_2, F_3, F_4.

2.3.2 Problem Constraints

This sub-section presents the equality and inequality restrictions related to the addressed problem as follows:

2.3.2.1 Equality Constraints

The balance between power generation and consumption is defined by [26-28]:

$$P_S(t) + \sum_{i=1}^{N_{PV}} P_{PV,i}(t) + \sum_{i=1}^{N_{WT}} P_{WT,i}(t) + \sum_{i=1}^{N_{Ele}} P_{Ele,i}(t) + \sum_{i=1}^{N_{FC}} P_{FC,i}(t) = \sum_{i=1}^{NT} P_{Loss,i}(t) + \sum_{i=1}^{NB} P_{Load,i}(t) \tag{2.32}$$

$$Q_S(t) + \sum_{i=1}^{N_{WT}} Q_{WT,i}(t) = \sum_{i=1}^{NT} Q_{Loss,i}(t) + \sum_{i=1}^{NB} Q_{Load,i}(t) \tag{2.33}$$

where the various components contribute to the system power balance at time t. $Q_S(t)$ and $P_S(t)$ denote the system reactive and active power supply, respectively. Additionally, real power from photovoltaic systems, wind turbines, electrolyzers, and fuel cells are considered by $P_{PV,i}(t), P_{WT,i}(t), P_{Ele,i}(t)$, and $P_{FC,i}(t)$, respectively. $Q_{WT,i}(t)$ represents the reactive power of wind turbines. Power losses are represented by $P_{Loss,i}(t)$ and $Q_{Loss,i}(t)$ for active and reactive powers, while $Q_{Load,i}(t)$ and $P_{Load,i}(t)$ reflect the reactive and active power required by load at node i and time t.

2.3.2.2 Inequality Constraints

a. Line Capacity Constraint

$$I_i \leq I_{Up,i} \tag{2.34}$$

where $I_{Up,i}$ defines the upper limit of current that the i^{th} line can safely carry, and I_i defines the current passing through each line of the studied DN.

b. Voltage Constraint

To maintain the stability, the voltage at each node must remain between 0.90 p.u. and 1.05 p.u.:

$$V_{Lp} \leq V_{(i,t)} \leq V_{Up} \tag{2.35}$$

where V_{Lp} represents the lower voltage limit, and V_{Up} represents the upper voltage limit, ensuring that the voltage $V_{(i,t)}$at node *i* and time *t* remains within this defined range.

c. WT's Power Factor Constraint

$$PF_{Lp} \leq PF_i \leq PF_{Up} \qquad i = 1,2,\dots,N_{WT} \tag{2.36}$$

where PF_{Lp} and PF_{Up} represent the lower and upper bounds of the power factor, respectively.

d. PV and WT Constraints

$$\sum_{i=1}^{N_{PV}} P_{PV\_rated,i} + \sum_{i=1}^{NN_{WT}} P_{WT\_rated,i} \leq \sum_{i=1}^{NB} P_{Load,i} \tag{2.37}$$

$$\sum_{i=1}^{N_{WT}} Q_{WT,i} \leq \sum_{i=1}^{NB} Q_{Load,i} \tag{2.38}$$

2.4 Optimization

In modern power systems, optimization plays a central role in ensuring efficient, reliable, and cost-effective operation, especially when integrating renewable energy sources and green hydrogen technologies. The complexity of such systems, driven by nonlinear relationships, variable energy inputs, and multiple design constraints, requires the use of powerful and flexible optimization techniques.

In this work, the Harris Hawks Optimization (HHO) algorithm was selected due to its strong global search capabilities, adaptive behaviour, and successful performance in solving a wide range of engineering problems. Inspired by the cooperative hunting strategy of Harris hawks in nature, this metaheuristic algorithm balances exploration and exploitation phases to converge towards optimal or near optimal solutions. This section details HHO's application for optimizing distribution networks with photovoltaic (PV), wind turbines, and hydrogen-based systems.

2.4.1 What is Optimization?

Optimization involves finding the best possible solution from a set of available alternatives by maximizing or minimizing a specific objective function (figure 2.1). This function is used to evaluate and compare different scenarios in order to determine which one yields the most favorable outcome in a given context [29].

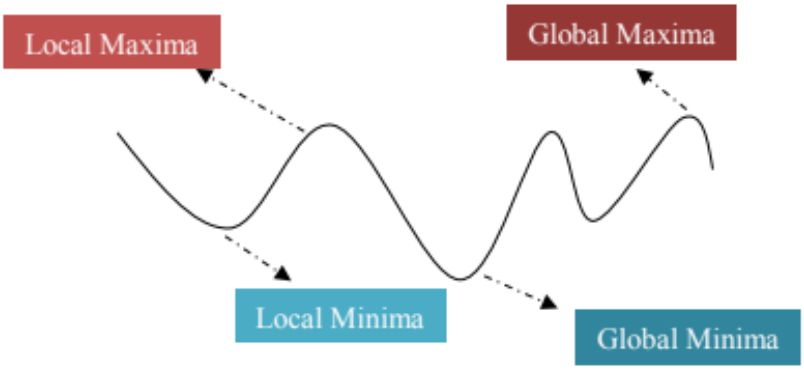

Figure 2.1 Local and global optimal solution

Typical applications of optimization include cost minimization, profit maximization, optimal system design, best approximations, and efficient control or resource management strategies.

2.4.2 Meta-Heuristics

In recent years, the development of optimization algorithms has been significantly influenced by natural phenomena, particularly biological behaviours. Bio inspired meta-heuristic optimization strategies provide promising avenues for obtaining near-optimal solutions in highly nonlinear and multidimensional search spaces. These methods tend to simplify the optimization process and perform more efficiently than conventional algorithms [29].

Generally, a heuristic refers to an approach based on trial and error, aiming to find satisfactory solutions without guaranteeing optimality. The prefix meta, meaning “beyond”, implies that meta-heuristics go beyond basic heuristics by incorporating more sophisticated strategies. A key characteristic of meta-heuristic algorithms is the use of randomness, which enables them to switch from local search to global search. This capability makes them particularly well suited for global optimization problems, even though they do not guarantee the discovery of the exact global optimum. Instead, they aim to provide good, feasible solutions within a reasonable time frame [29].

Most meta-heuristic algorithms are structured around two fundamental components: diversification and intensification also known respectively as exploration and exploitation. Diversification refers to the ability of the algorithm to explore the search space broadly and generate a wide variety of solutions. Intensification focuses the search in promising regions

where high-quality solutions have already been found, refining them further. Therefore, when selecting the optimal solution, it is essential to strike a proper balance between diversification and intensification. Achieving this balance improves the convergence rate of the algorithm and enhances the chances of reaching a globally optimal solution [29]. In this study, we apply the Harris Hawks Optimization (HHO) algorithm, which belongs to the family of swarm based meta-heuristic methods.

2.4.3 Harris Hawks Optimization

Harris Hawks Optimization (HHO) is a recent population-based, nature-inspired metaheuristic algorithm introduced in 2019 and published in Future Generation Computer Systems [29]. The algorithm draws its inspiration from the cooperative hunting behaviour of Harris hawks in the wild, particularly a strategy known as the “surprise pounce” or the “seven kills” technique.

In this strategy, a group of hawks coordinates a series of rapid, strategic attacks from multiple directions to confuse and exhaust their prey (figure 2.1). While a successful capture can sometimes be achieved within seconds, prey that actively resists may force the hawks to perform several short, intense dives over a few minutes. This behaviour reflects a dynamic and adaptive approach to pursuit, where the hawks adjust their tactics based on the prey’s reactions.

The strength of this cooperative method lies in its ability to wear down the target. By continuously pressuring and disorienting the prey, the hawks reduce its ability to escape or recover, ultimately making it more vulnerable. Eventually, one of the hawks seizes the opportunity to capture the exhausted prey.

Figure 2.1 Harris Hawks detecting and chasing the prey

HHO translates this intelligent hunting behaviour into a mathematical model designed for solving complex optimization problems. The algorithm simulates various attack phases and movement patterns to explore and exploit the search space efficiently [29].

2.4.3.1 Harris Hawks Optimization Phases

a. Exploration Phase

In HHO, the Harris' hawks perch randomly on some locations and wait to detect a prey based on two strategies:

$$X(t+1) = f(x) = \begin{cases} X_{rand}(t) - r_1 |X_{rand}(t) - 2r_2 X(t)| & q \geq 0.5 \\ (X_{rabbit}(t) - X_m(t)) - r_3(LB + r_4(UB - LB)) & q < 0.5 \end{cases} \quad (2.39)$$

In the Harris Hawks Optimization algorithm, $X(t+1)$ represents the updated position vector of a hawk at iteration *t+1*, while *X(t)* denotes its current position. The term $X_{rabbit}(t)$ corresponds to the estimated position of the prey at iteration t, which guides the search process toward the global optimum.

Several random numbers r_1, r_2, r_3, r_4 and q are generated within the range (0,1) and are refreshed at each iteration to introduce stochastic behavior into the algorithm.

Additionally, $X_{rand}(t)$ refers to the position of a randomly selected hawk from the current population, used to introduce variation and diversity. $X_m(t)$ represents the mean position of the entire hawk population at iteration t, contributing to the collaborative nature of the search.

The variables *LB* and *UB* define the lower and upper bounds of the solution space, ensuring that the hawks' positions remain within feasible limits during the optimization process.

b. Transition from Exploration to Exploitation

The energy of a rabbit is modeled as:

$$E = 2E_0\left(1 - \frac{t}{T}\right) \quad (2.40)$$

E indicates the escaping energy of the prey; T is the maximum number of iterations and E_0 is the initial state of its energy.

c. Exploitation Phase

- **Soft besiege**

$$X(t+1) = \Delta X(t) - E\ |JX_{rabbit}(t) - X(t)| \quad (2.41)$$

Here, $\Delta X(t)$ denotes the difference between the rabbit's position and the current hawk position at iteration t. This term reflects the directional distance that guides the hawk's movement toward the prey.

J represents the random jump strength of the rabbit during the escape process. Its value is randomly updated in each iteration to mimic the unpredictable and dynamic motion patterns of a real rabbit in nature.

- **Hard besiege**

The current positions are updated using:

$$X(t+1) = X_{rabbit}(t) - E\ |\Delta X(t)| \tag{2.42}$$

- **Soft besiege with progressive rapid dives**

To carry out the soft besiege phase, it is assumed that the hawks are capable of evaluating and selecting their next move according to the rule defined in Equation. This decision-making process allows them to gradually approach the prey without launching an immediate aggressive attack.

$$Y = X_{rabbit}(t) -\ E\ |JX_{rabbit}(t) - X(t)| \tag{2.43}$$

In this scenario, it is further assumed that the hawks perform dives using Lévy flight-based movement patterns, as governed by the rule provided in Equation.

$$Z = Y + S \times LF(D) \tag{2.44}$$

D represents the dimension of the problem, *S* is a random vector of size 1×D, and *LF* refers to the Lévy flight distribution function. Accordingly, the complete strategy for updating the hawks' positions during the soft besiege phase is described in Equation.

$$X(t+1) = \begin{cases} Y\ if\ F(Y) < F(X(t)) \\ Z\ if\ F(Z) < F(X(t)) \end{cases} \tag{2.45}$$

- **Hard besiege with progressive rapid dives**

In the hard besiege phase, the hawks' movement is governed by the strategy defined in Equations (2.46 and 2.47).

$$X(t+1) = \begin{cases} Y\ if\ F(Y) < F(X(t)) \\ Z\ if\ F(Z) < F(X(t)) \end{cases} \tag{2.46}$$

The intermediate position vectors Y and Z, used during this phase, are calculated based on the updated rules outlined in Equations.

$$Y = X_{rabbit}(t) - E\ |JX_{rabbit}(t) - X_m(t)|$$
$$Z = Y + S \times LF(D) \tag{2.47}$$

2.4.4 Evaluation of the HHO Algorithm

- Simple Structure and Easy Implementation: HHO has a straightforward design with only a single control parameter (energy parameter E) that balances exploration and exploitation, making it easy to implement.
- Adaptive and Time-Varying Search: The algorithm adapts its search behavior over iterations, helping it to avoid some local minima and better explore the search space.
- Versatility: HHO has been successfully applied in diverse fields such as power system engineering, wireless networks, feature selection, and meta grating design, showing good adaptability to different problem types.
- Promising Results Compared to Other Metaheuristics: In some studies, HHO outperforms classical algorithms like Particle Swarm Optimization (PSO), Genetic Algorithm (GA), and Differential Evolution (DE) in finding Pareto-optimal fronts and global optima.

2.5 Conclusion

This chapter provided a comprehensive overview of the key components involved in the optimal operation of a hybrid distribution network integrating green hydrogen technologies. It began by introducing the fundamentals and operational principles of green hydrogen systems, including photovoltaic (PV) panels, wind turbines (WT), electrolyzers, and hydrogen storage units. A detailed problem formulation was then presented, defining four objective functions aiming to minimize real power losses, operation costs, voltage deviation, and pollutant emissions. The corresponding decision variables and operational constraints were also established to ensure both technical feasibility and regulatory compliance. Following the formulation, the Harris Hawks Optimization (HHO) algorithm was introduced as the selected optimization tool. Its nature inspired logic and dynamic exploration exploitation behaviour make it well suited for solving complex multi-objective problems within hybrid energy systems. Altogether, this chapter laid the mathematical and methodological foundation for the next phase of the work, where simulation scenarios will be conducted to evaluate the performance of the proposed model. These results will help demonstrate the techno-economic and environmental benefits of integrating green hydrogen systems into modern distribution networks.

Chapter III

Optimal Operation of DN Integrating GHS for Techno-Economic and Environmental Benefits

3.1 Introduction

This chapter addresses the optimal siting and sizing of Renewable Energy Resources (RERs) and green hydrogen storage systems under three distinct operational scenarios. The first scenario, representing the base case, assumes the absence of both RERs and hydrogen-based components. The second scenario involves the integration of RERs only, while the third scenario considers the simultaneous integration of both RERs and green hydrogen technologies. The analysis includes the optimal integration of photovoltaic (PV) units, wind turbines (WTs), electrolyzers, hydrogen storage tanks, and fuel cells. The Harris Hawks Optimization (HHO) algorithm is employed to determine the optimal locations and capacities of these components, as well as the optimal power factor for wind turbines. The test system used in this study is the standard IEEE 33-bus electrical distribution network, and the power flow calculations are performed using the backward-forward sweep method. The simulation framework is implemented in MATLAB 2021a and executed on a system equipped with an Intel Core i7-3537U processor (2.5 GHz) and 6 GB of RAM. The subsequent section presents and discusses the simulation results for the defined scenarios. The proposed optimization approach uses a fixed population size of 20 and a maximum of 40 iterations. This chapter builds upon the multi-objective optimization framework outlined in the previous chapter, targeting technical, economic, and environmental performance indicators while assessing the effectiveness of the HHO algorithm in solving such complex problems.

3.2 Description of the Test System

The proposed optimization framework was implemented and evaluated on the IEEE 33-bus radial distribution network, a widely recognized benchmark in power system analysis. This network represents a medium-voltage distribution feeder and is characterized by a relatively high resistance-to-reactance ratio and structural complexity, making it well-suited for assessing power flow algorithms and distributed generation integration strategies [30]. In this study, the network was modeled under normal operating conditions, without any topological reconfiguration, and was assumed to operate based on a 24-hour load profile and time-varying electricity prices. Additionally, the system was subjected to daily weather variations, as illustrated in the figure 3.1.

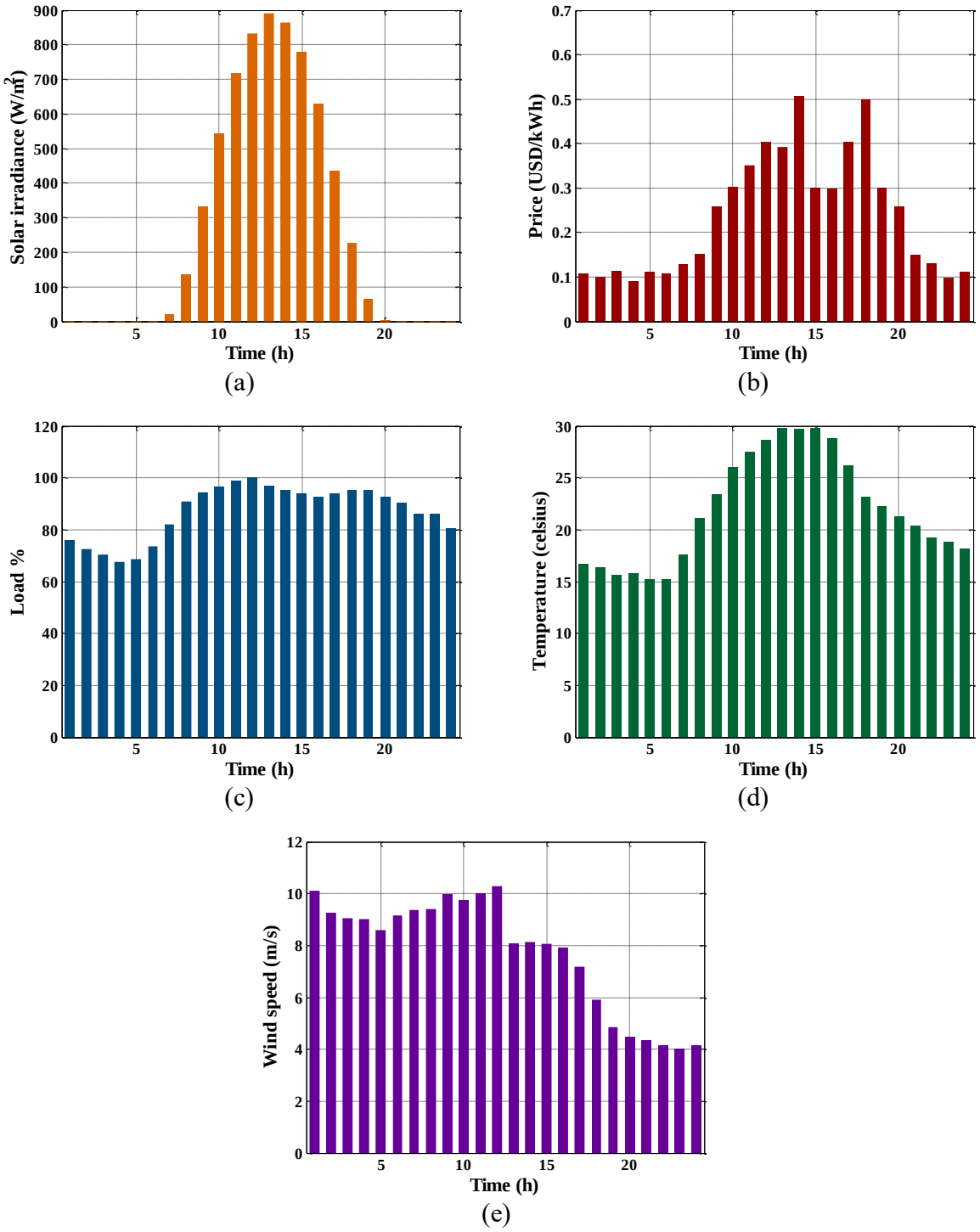

Figure 3.1 Variation of data over 24 hours: (a) solar irradiance, (b) electricity price, (c) load percentage, (d) temperature, and (e) wind speed

The test system, as shown in the figure 3.2, is used to simulate various operating scenarios to evaluate the technical, economic, and environmental impacts of hybrid energy integration.

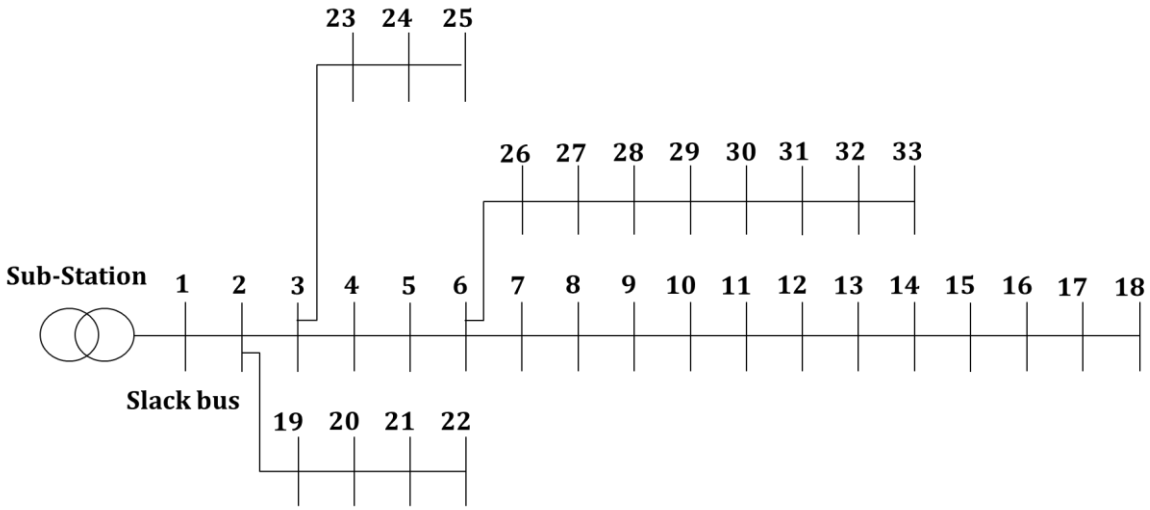

Figure 3.2 Schematic diagram of the IEEE 33-bus EDN

Table 3.1 presents the selected limits of system voltage, as well as the number of PV panels, wind turbine units, electrolyzers, hydrogen tanks, and fuel cells. It also includes the power factor of the wind turbine generators. Each PV panel provides 255 W, each wind turbine delivers 250 kW, each electrolyzer works between 1 kW to 6.2 kW, each fuel cell generates 6 kW, and each hydrogen tank stores 100 kWh.

Table 3.1 Grid and generators constraints

Generator and grid constraints	Value
Bounds of voltage	$0.9\,p.u \leq V \leq 1.05\,p.u$
Number of PV panels	$0 \leq \text{panels} \leq 100000$ panels
Number of WTs	$0 \leq \text{WT} \leq 90$ turbines
Number of electrolyzers	$0 \leq \text{electrolyzers} \leq 100$ electrolyzers
Number of hydrogen tanks	$0 \leq \text{tanks} \leq 100$ tanks
Number of fuel cells	$0 \leq \text{fuel cells} \leq 100$ fuel cells
WT's power factor	$0.7 \leq PF \leq 1$

3.3 Simulation Results and Analysis

The simulation model was implemented in MATLAB, which offers a robust and flexible environment for power system modeling and optimization. The developed program is based on the mathematical formulations introduced in Chapter 2, including the objective functions and system constraints relevant to the problem. To evaluate the impact of integrating renewable

energy sources and green hydrogen systems into the distribution network, three distinct operating scenarios were defined. Each scenario represents a different configuration of energy sources and system components. The same IEEE 33 bus radial distribution system and 24-hour simulation horizon were used in all cases to ensure a consistent basis for comparison.

3.3.1 Scenario 1: Base Case

This scenario represents the reference configuration in which all loads are supplied exclusively by the main grid. No photovoltaic systems, wind turbines, or hydrogen-based components are included, reflecting the conventional operation of a distribution system. After applying the backward-forward sweep algorithm, the daily results for power loss, grid power, voltage deviation, and emissions are illustrated in the figure 3.3.

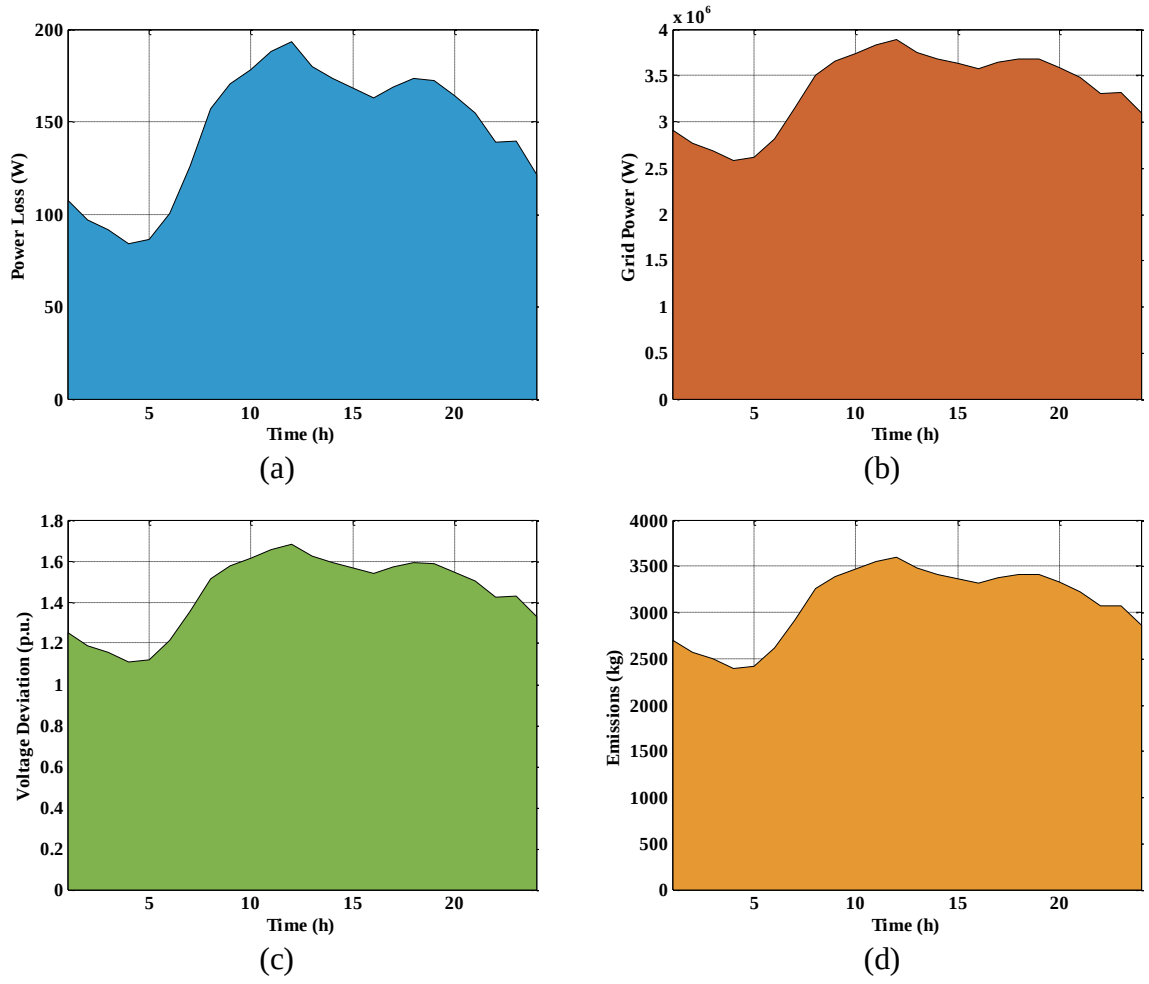

Figure 3.3 Daily results in the base case: (a) power loss, (b) grid power, (c) voltage deviation, and (d) emissions

The table 3.2 presents the detailed daily results for Scenario #1, including technical, economic, and environmental performance indicators. As this scenario represents the base case without any integrated renewable or hydrogen-based components, the optimal sizing and placement parameters are not applicable.

Table 3.2 Technical, Economic, and Emission Results for Scenario #1

Item		**Scenario #1**
Technical results	Power losses (W)	3495.6407
	Voltage deviation (p.u)	34.7368
Economic results	Total cost (USD/kWh)	20080.1211
Emission results	Total emission (kg)	74667.6484
Optimal location	Bus	---
Optimal P.F	Wind turbine	---
Optimal size	Photovoltaic (kW)	---
	Wind turbine (kW)	---
	Electrolyzer (kW)	---
	Fuel cell (kW)	---

3.3.2 Scenario 2: Integration of PV and Wind Energy

In this scenario, distributed renewable energy sources are integrated into the system. Photovoltaic panels and wind turbines are installed at selected buses to partially supply the load demand. The objective is to evaluate the impact of renewable energy integration on power losses, voltage deviation, operational costs, and emissions. The results of these daily performance indicators are illustrated in the figure 3.4.

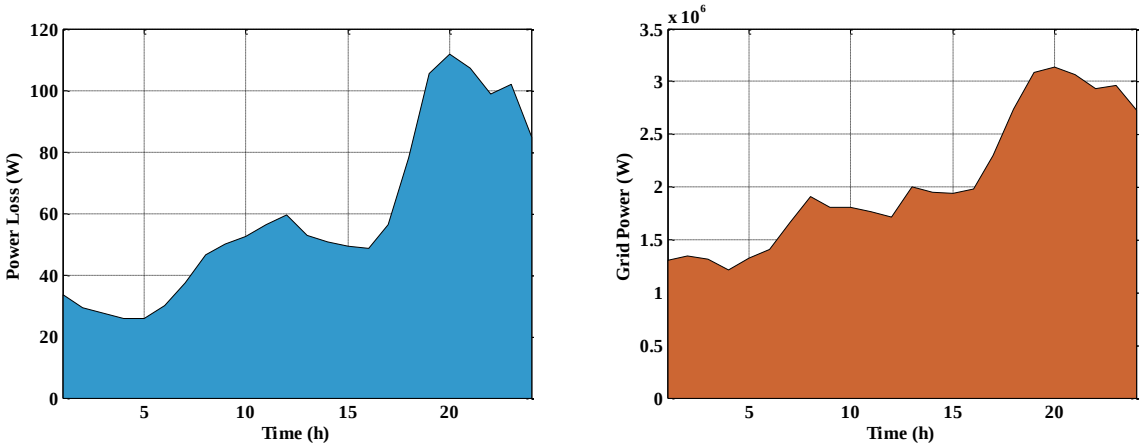

(a) (b)

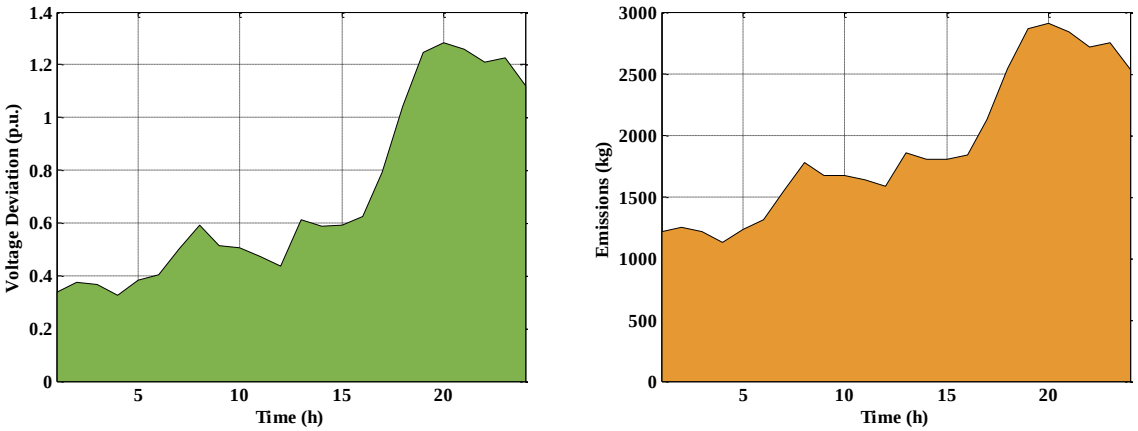

(c) (d)

Figure 3.4 Daily results in the Scenario #2: (a) power loss, (b) grid power, (c) voltage deviation, and (d) emissions

Table 3.3 presents the technical, economic, and emission results for Scenario #2, in which photovoltaic systems and wind turbines are integrated into the distribution network. This scenario aims to assess the effect of incorporating distributed renewable energy sources without hydrogen-based components on the overall system performance.

Table 3.3 Technical, Economic, and Emission Results for Scenario #2

Item		**Scenario #2**
Technical results	Power losses (W)	1420.0160
	Voltage deviation (p.u)	16.8060
Economic results	Total cost (USD/kWh)	12065.2601
Emission results	Total emission (kg)	45796.0276
Optimal location	Bus	28
Optimal P.F	Wind turbine	0.76
Optimal size	Photovoltaic (kW)	500
	Wind turbine (kW)	2500
	Electrolyzer (kW)	---
	Fuel cell (kW)	---
MOF		0.44

As shown in Table 3.3, the integration of renewable energy sources in Scenario #2 has resulted in significant improvements across all evaluated performance metrics compared to the base case. Specifically, the total power losses have decreased markedly to 1420.0160 W, and the voltage deviation has been reduced to 16.8060 p.u., indicating improved voltage regulation and enhanced network efficiency. From an economic standpoint, the total operational cost has declined to 12065.2601 USD/kWh, demonstrating the cost-effectiveness of utilizing local renewable generation to reduce reliance on grid-supplied electricity. In addition, the total

emissions have dropped to 45796.0276 kg, confirming the positive environmental impact of renewable energy integration. The optimization process identified bus 28 as the optimal location for the placement of distributed generation units, while the optimal power factor for the wind turbine is determined to be 0.76, ensuring appropriate reactive power compensation. The deployed renewable capacities include 500 kW of photovoltaic generation and 2500 kW of wind turbine capacity. No hydrogen-based components (electrolyzers or fuel cells) were installed in this scenario, as indicated by the absence of corresponding values in the table. The overall effectiveness of this configuration is reflected in the MOF value of 0.44, supporting the conclusion that the integration of renewable energy sources alone can significantly enhance the technical, economic, and environmental performance of distribution networks.

3.3.3 Scenario 3: Integration of Green Hydrogen System

The third scenario includes the same photovoltaic and wind energy sources as in Scenario 2, with the addition of a green hydrogen system consisting of an electrolyzer, fuel cells, and hydrogen storage. Excess renewable energy is utilized to produce hydrogen, which is stored and later converted back into electricity when needed. The results of this scenario are presented in Figure 3.5.

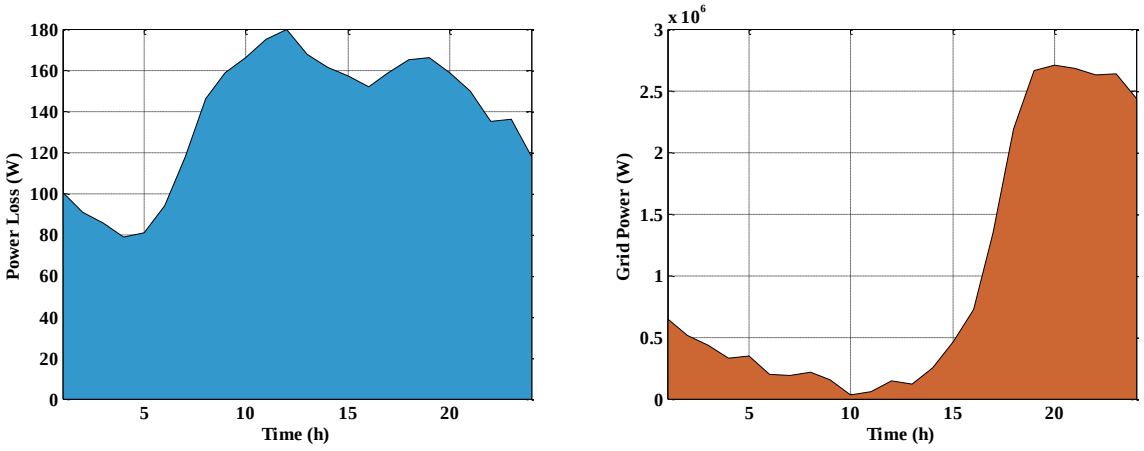

(a) (b)

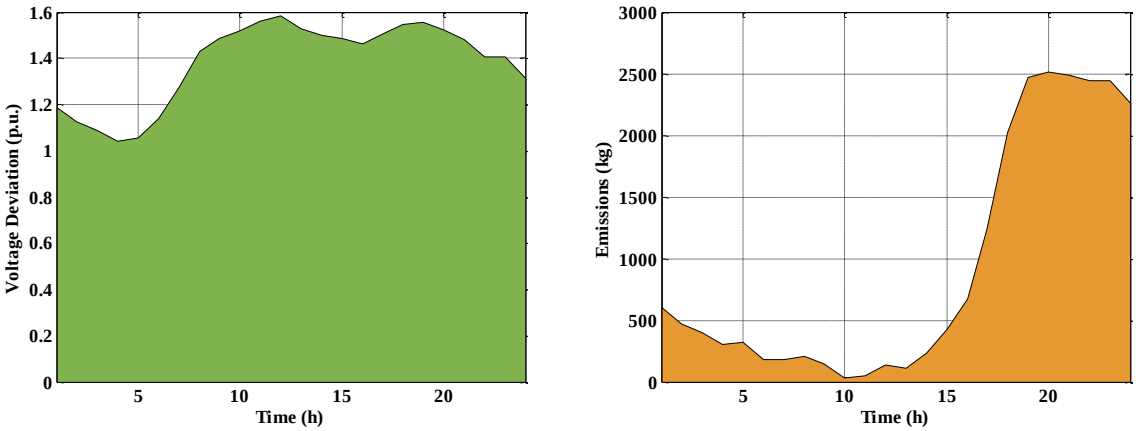

(c) (d)

Figure 3.5 Daily results in the Scenario #3: (a) power loss, (b) grid power, (c) voltage deviation, and (d) emissions

To validate the charging and discharging process of the hydrogen storage system, it is essential to assess the State of Charge (SOC), as shown in the figure 3.6. The results indicate that the storage system is charged using excess power during hours 9, 10, 11, 12, and 13, confirming the presence of surplus energy during this period. Conversely, the system discharges (supplies energy) during hours 14 and 15, demonstrating its role in supporting the load when renewable generation is insufficient.

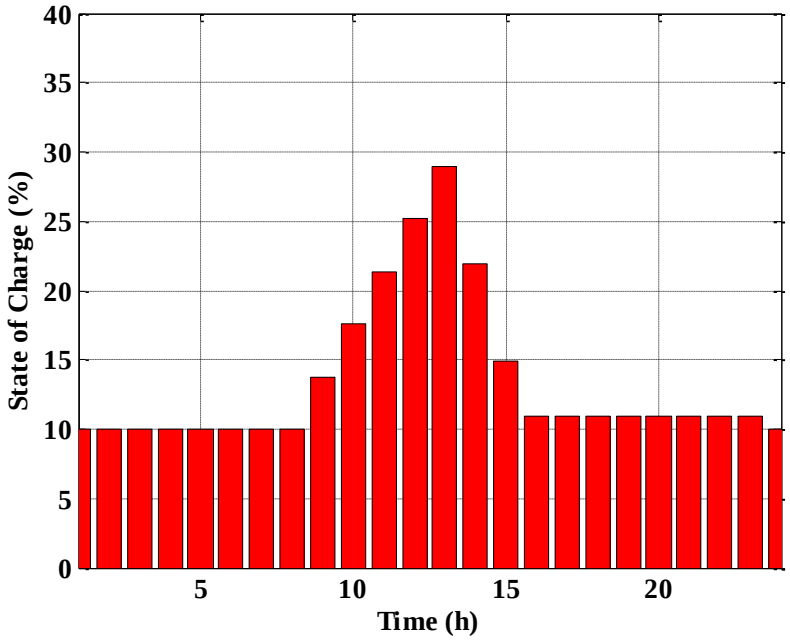

Figure 3.6 State of charge result of green hydrogen system

Table 3.4 presents the technical, economic, and environmental results for Scenario #3, which considers the integration of renewable energy sources along with a green hydrogen system composed of an electrolyzer, fuel cells, and hydrogen storage. This configuration is designed to utilize excess renewable energy for hydrogen production, which can later be converted back into electricity when needed.

Table 3.4 Technical, Economic, and Emission Results for Scenario #3

Item		**Scenario #3**
Technical results	Power losses (W)	3298.7023
	Voltage deviation (p.u)	33.1971
Economic results	Total cost (USD/kWh)	10262.3948
Emission results	Total emission (kg)	22332.0587
Optimal location	Bus	2
Optimal P.F	Wind turbine	0.7
Optimal size	Photovoltaic (kW)	2805
	Wind turbine (kW)	2250
	Electrolyzer (kW)	6.2
	Fuel cell (kW)	6
MOF		0.6762

In this scenario, the system demonstrates a balance between the benefits of renewable integration and the added flexibility provided by hydrogen storage. The power losses amount to 3298.7023 W, which, although higher than Scenario #2 (without hydrogen), remain lower than the base case (Scenario #1), indicating a moderate trade-off due to the added complexity of hydrogen components. The voltage deviation is 33.1971 p.u., slightly improved compared to the base case but higher than the renewable-only scenario, reflecting some voltage regulation challenges introduced by hydrogen system operation. Economically, this scenario shows a significant reduction in cost compared to both previous scenarios. The total operational cost is minimized to 10262.3948 USD/kWh, showcasing the economic advantage of using stored energy from hydrogen during high-price periods. In addition, total emissions are drastically reduced to 22332.0587 kg, the lowest among all scenarios, highlighting the environmental effectiveness of combining renewable energy with hydrogen storage. The optimal location for system deployment is identified as bus 2, and the optimal power factor for the wind turbine is 0.7, ensuring efficient reactive power management. The optimal sizes for each component include 2805 kW of PV capacity, 2250 kW of wind turbine capacity, 6.2 kW for the electrolyzer, and 6 kW for the fuel cell. This configuration allows efficient energy conversion, storage, and dispatch, especially under variable load and generation conditions. Finally, MOF value is

0.6762, which, while higher than in Scenario #2, reflects a balanced trade-off between technical performance, cost savings, and emission reductions.

3.4 Conclusion

In this chapter, the optimal operation of a distribution network integrating photovoltaic, wind, and green hydrogen systems was investigated through three scenarios. The first scenario represented the conventional base case, while the second incorporated only renewable energy sources. The third scenario combined renewables with a green hydrogen storage system. Simulation results demonstrated that integrating renewable energy significantly improves the technical, economic, and environmental performance of the network. Furthermore, adding hydrogen-based components provided additional flexibility, reduced emissions, and lowered overall operational costs. The Harris Hawks Optimization (HHO) algorithm effectively identified optimal sizes, locations, and power factors for system components under each scenario. These results confirm the value of hybrid renewable-hydrogen integration for sustainable and efficient power distribution.

General Conclusion

This master's thesis has presented a comprehensive study on the optimal integration of renewable energy sources (RES) and green hydrogen storage systems (GHS) into electrical distribution networks (EDNs). Through advanced modeling, simulation, and optimization techniques, the research aimed to enhance the technical performance, economic efficiency, and environmental sustainability of future distribution systems.

A thorough analysis of distribution network characteristics highlighted the limitations of conventional power flow methods in radial systems. The Backward/Forward Sweep (BFS) algorithm was adopted to accurately model power flows under realistic load and topology conditions.

Dynamic models for photovoltaic (PV) panels, wind turbines (WTs), and hydrogen-based components (electrolyzer, fuel cell, and storage tank) were developed, enabling realistic interaction with the grid.

A multi-objective optimization problem was formulated, minimizing total real power losses, operational costs, voltage deviations, and pollutant emissions. The Harris Hawks Optimization (HHO) algorithm was employed to solve the problem efficiently.

Case studies using the IEEE 33-bus test system validated the proposed approach under three scenarios:

- **Scenario 1 (Base Case):** Conventional operation relying solely on grid-supplied energy.
- **Scenario 2 (RES only):** Integration of PV and wind energy, achieving a 59% reduction in power losses and 39% lower emissions.
- **Scenario 3 (RES + GHS):** Integration of green hydrogen components, resulting in the highest emission reduction (70%), cost savings (49%), and improved voltage regulation.

The transition to low-carbon, resilient energy systems depends on the strategic deployment of renewables and storage within distribution networks. This thesis has demonstrated that the combined use of RES and green hydrogen storage not only reduces technical losses and emissions but also enhances grid stability and cost-effectiveness. The models, methods, and insights developed in this research offer a valuable roadmap for future

innovations in energy distribution, contributing to global decarbonization goals and a sustainable energy future. These results confirm the technical viability and economic-environmental benefits of hybrid renewable-hydrogen systems in EDNs.

Limitations and Future Work

While the current work provides a solid foundation, several directions are recommended for future research:

- ✓ The current study was conducted over a 24-hour period. Extending the simulation to cover an entire year considering seasonal variations in demand, solar irradiance, and wind availability could provide deeper insights and likely yield even more favorable and realistic results in terms of system performance and economic return.
- ✓ Developing hybrid metaheuristic methods that combine HHO with artificial intelligence or machine learning could improve optimization speed and solution accuracy for large-scale systems.
- ✓ Incorporating probabilistic models for RES output and load demand would improve robustness under variable and unpredictable conditions.
- ✓ Investigating combinations of hydrogen with other storage systems (e.g., batteries or supercapacitors) may enhance short- and long-term operational flexibility.

References

References

[1] D. Singh, D. Singh, and K. Verma, "Multiobjective optimization for DG planning with load models," *IEEE transactions on power systems,* vol. 24, no. 1, pp. 427-436, 2009.

[2] K. D. Singh and S. Ghosh, "A new efficient method for load-flow solution for radial distribution networks," *Electrical Review, pe. org. pl/articles/2011/12a,* pp. 66-73, 2011.

[3] M. Srinivas, "Distribution load flows: a brief review," in *2000 IEEE Power Engineering Society Winter Meeting. Conference Proceedings (Cat. No. 00CH37077)*, 2000, vol. 2: IEEE, pp. 942-945.

[4] U. Eminoglu and M. H. Hocaoglu, "Distribution systems forward/backward sweep-based power flow algorithms: a review and comparison study," *Electric Power Components and Systems,* vol. 37, no. 1, pp. 91-110, 2008.

[5] A. G. Expósito and E. R. Ramos, "Reliable load flow technique for radial distribution networks," *IEEE Transactions on Power Systems,* vol. 14, no. 3, pp. 1063-1069, 1999.

[6] U. Eminoglu and M. H. Hocaoglu, "A new power flow method for radial distribution systems including voltage dependent load models," *Electric power systems research,* vol. 76, no. 1-3, pp. 106-114, 2005.

[7] G. Chang, S. Chu, and H. Wang, "An improved backward/forward sweep load flow algorithm for radial distribution systems," *IEEE Transactions on power systems,* vol. 22, no. 2, pp. 882-884, 2007.

[8] J. Liu, M. Salama, and R. Mansour, "An efficient power flow algorithm for distribution systems with polynomial load," *International Journal of Electrical Engineering Education,* vol. 39, no. 4, pp. 371-386, 2002.

[9] A. Alsaadi and B. Gholami, "An effective approach for distribution system power flow solution," *International Journal of Electrical and Computer Engineering,* vol. 3, no. 1, pp. 1-5, 2009.

[10] P. M. De Oliveira-De Jesus, "The Standard Backward/Forward Sweep Power Flow."

[11] N. Goudarzi and W. Zhu, "A review of the development of wind turbine generators across the world," in *ASME International Mechanical Engineering Congress and Exposition*, 2012, vol. 45202: American Society of Mechanical Engineers, pp. 1257-1265.

[12] A. T. Hachemi *et al.*, "Modified reptile search algorithm for optimal integration of renewable energy sources in distribution networks," *Energy Science & Engineering,* vol. 11, no. 12, pp. 4635-4665, 2023.

[13] A. Mewafy, I. Ismael, S. S. Kaddah, W. Hu, Z. Chen, and S. Abulanwar, "Optimal design of multiuse hybrid microgrids power by green hydrogen–ammonia," *Renewable and Sustainable Energy Reviews,* vol. 192, p. 114174, 2024.

[14] R. Dufo-Lopez and J. L. Bernal-Agustín, "Multi-objective design of PV–wind–diesel–hydrogen–battery systems," *Renewable energy,* vol. 33, no. 12, pp. 2559-2572, 2008.

[15] R. Wang and R. Zhang, "Techno-economic analysis and optimization of hybrid energy systems based on hydrogen storage for sustainable energy utilization by a biological-inspired optimization algorithm," *Journal of Energy Storage,* vol. 66, p. 107469, 2023.

[16] A. Hachemi, F. Sadaoui, and S. Arif, "Optimal location and sizing of capacitor banks in distribution systems using grey wolf optimization algorithm," in *International Conference on Artificial Intelligence in Renewable Energetic Systems*, 2022: Springer, pp. 719-728.

[17] T. U. Badrudeen, F. K. Ariyo, and N. Nwulu, "Voltage stability improvement and power losses reduction through multiple grid contingency supports," *Energy Exploration & Exploitation,* p. 01445987231218292, 2024.

[18] S. Sultana and P. K. Roy, "Optimal capacitor placement in radial distribution systems using teaching learning based optimization," *International Journal of Electrical Power & Energy Systems,* vol. 54, pp. 387-398, 2014.

[19] S. R. Gampa and D. Das, "Optimum placement and sizing of DGs considering average hourly variations of load," *International Journal of Electrical Power & Energy Systems,* vol. 66, pp. 25-40, 2015.

[20] N. Augustine, S. Suresh, P. Moghe, and K. Sheikh, "Economic dispatch for a microgrid considering renewable energy cost functions," in *2012 IEEE PES Innovative Smart Grid Technologies (ISGT)*, 2012: IEEE, pp. 1-7.

[21] N. A. Nagem, M. Ebeed, D. Alqahtani, F. Jurado, N. H. Khan, and W. A. Hafez, "Optimal design and three-level stochastic energy management for an interconnected microgrid with hydrogen production and storage for fuel cell electric vehicle refueling stations," *International Journal of Hydrogen Energy,* vol. 87, pp. 574-587, 2024.

[22] A. Asaad *et al.*, "Multi-objective optimal planning of EV charging stations and renewable energy resources for smart microgrids," *Energy Science & Engineering,* vol. 11, no. 3, pp. 1202-1218, 2023.

[23] M. Purlu and B. E. Turkay, "Optimal allocation of renewable distributed generations using heuristic methods to minimize annual energy losses and voltage deviation index," *IEEE Access,* vol. 10, pp. 21455-21474, 2022.

[24] D. Ahmed *et al.*, "An enhanced jellyfish search optimizer for stochastic energy management of multi-microgrids with wind turbines, biomass and PV generation systems considering uncertainty," *Scientific Reports,* vol. 14, 2024.

[25] M. Esmaeili, M. Sedighizadeh, and M. Esmaili, "Multi-objective optimal reconfiguration and DG (Distributed Generation) power allocation in distribution networks using Big Bang-Big Crunch algorithm considering load uncertainty," *Energy,* vol. 103, pp. 86-99, 2016.

[26] M. A. Elseify, F. A. Hashim, A. G. Hussien, H. Abdel-Mawgoud, and S. Kamel, "Boosting prairie dog optimizer for optimal planning of multiple wind turbine and photovoltaic distributed generators in distribution networks considering different dynamic load models," *Scientific Reports,* vol. 14, no. 1, pp. 1-33, 2024.

[27] M. A.-E.-H. Mohamed, S. Kamel, M. M. Alrashed, and M. F. Elnaggar, "Power flow optimization in distribution networks: Estimating optimal distribution generators through pseudo-inverse analysis," *Energy Reports,* vol. 11, pp. 2935-2970, 2024.

[28] A. T. Hachemi, R. M. Kamel, M. Hashem, M. Ebeed, and A. Saim, "Reliability and line loading enhancement of distribution systems using optimal integration of renewable energy and compressed air energy storages simultaneously under uncertainty," *Journal of Energy Storage,* vol. 101, p. 113921, 2024.

[29] A. A. Heidari, S. Mirjalili, H. Faris, I. Aljarah, M. Mafarja, and H. Chen, "Harris hawks optimization: Algorithm and applications," *Future generation computer systems,* vol. 97, pp. 849-872, 2019.

[30] A. T. Hachemi, M. Ebeed, M. Hashem, F. Jurado, and A. Saim, "Techno-economic-environmental Assessment of Distribution Networks with Integrated PV Systems and D-STATCOMs Under Uncertainty," in *2024 25th International Middle East Power System Conference (MEPCON)*, 2024: IEEE, pp. 1-6.